

Global and local gray matter loss in mild cognitive impairment and Alzheimer's disease

G.B. Karas,^{a,b,c,*} P. Scheltens,^{b,c,d} S.A.R.B. Rombouts,^{c,e} P.J. Visser,^c
R.A. van Schijndel,^{b,e} N.C. Fox,^f and F. Barkhof^{ca,b,c}

^aDepartment of Diagnostic Radiology, Vrije Universiteit Medical Center, Amsterdam, The Netherlands

^bImage Analysis Center, Vrije Universiteit Medical Center, Amsterdam, The Netherlands

^cAlzheimer Center, Vrije Universiteit Medical Center, Amsterdam, The Netherlands

^dDepartment of Clinical Neurology, Vrije Universiteit Medical Center, Amsterdam, The Netherlands

^eDepartment of Clinical Physics and Informatics, Vrije Universiteit Medical Center, Amsterdam, The Netherlands

^fDementia Research Group, Department of Clinical Neurology, Institute of Neurology, Queen Square, London, England, UK

Received 21 March 2004; revised 2 June 2004; accepted 2 July 2004
Available online 13 August 2004

Purpose. Mild cognitive impairment (MCI) is thought to be the prodromal phase to Alzheimer's disease (AD). We analyzed patterns of gray matter (GM) loss to examine what characterizes MCI and what determines the difference with AD.

Materials and methods. Thirty-three subjects with AD, 14 normal elderly controls (NCLR), and 22 amnesic MCI subjects were included and underwent brain MR imaging. Global GM volume was assessed using segmentation and local GM volume was assessed using voxel-based morphometry (VBM); VBM was optimized for template mismatch and statistical mass.

Results. AD subjects had significantly (12.3%) lower mean global GM volume when compared to controls (517 ± 58 vs. 590 ± 52 ml; $P < 0.001$). Global GM volume in the MCI group (552 ± 52) was intermediate between these two: 6.2% lower than AD and 6.5% higher than the controls but not significantly different from either group. VBM showed that subjects with MCI had significant local reductions in gray matter in the medial temporal lobe (MTL), the insula, and thalamus compared to NCLR subjects. By contrast, when compared to subjects with AD, MCI subjects had more GM in the parietal association areas and the anterior and the posterior cingulate.

Conclusion. GM loss in the MTL characterizes MCI, while GM loss in the parietal and cingulate cortices might be a feature of AD.

© 2004 Elsevier Inc. All rights reserved.

Keywords: Voxel-based morphometry; Computational neuroanatomy; Alzheimer's disease; Mild cognitive impairment

Introduction

Mild cognitive impairment (MCI) is a clinical term describing the transitional state between normal aging and dementia (Petersen et al., 2001). Patients with amnesic MCI are characterized by isolated episodic memory loss greater than expected by age alone, but not enough to meet criteria for probable Alzheimer's disease (AD) (McKhann et al., 1984). Recent MRI research in MCI shows atrophy of the parahippocampal gyrus and medial temporal lobe (MTL) in one study (Visser et al., 1999), and of the entorhinal cortex, the banks of the superior temporal sulcus, and the anterior cingulate in another (Killiany et al., 2000) compared to controls. The choice of which structure to measure is likely to have been guided by histopathological staging research, which particularly identifies the medial temporal lobe as being involved early in AD (Braak and Braak, 1991; Delacourte et al., 1999). It has been recognized though that there might be a discrepancy between amyloid deposition, tangle formation, and neuronal loss: Neuronal loss is greater than what would be expected from direct amyloid damage alone (Gomez-Isla et al., 1997) and that might be reflected on gray matter loss (GML) on MRI. Likewise, in vivo measures of hypometabolism in the brain appear to follow a different pattern than the histopathological (Braak) stages (De Santi et al., 2001; Mega et al., 1997; Mega et al., 1999). Loss of synaptic neurotrophic support might lead cortical areas in the brain to exhibit atrophy earlier than would have been anticipated neuropathologically (Braak and Braak, 1991; Smith, 2002a). In other words, extrapolating neuropathological findings to describe AD and its prodromal stages introduces a certain degree of bias toward conformance to the Braak staging. A recent study attempted to correct for the bias and identify atrophic regions in MCI vs. AD (Chetelat et al., 2002). In that study, the authors used a statistical framework based on local statistical maxima to highlight GML

* Corresponding author. PO Box 7057, 1007 MB, Amsterdam, The Netherlands. Fax: +31 20 4041945.

E-mail address: GB.Karas@vumc.nl (G.B. Karas).

Available online on ScienceDirect (www.sciencedirect.com.)

throughout the whole brain but failed to find hippocampal volume differences between MCI and AD. To tackle the methodological issues and assess the suggestion (Chetelat et al., 2002) of a lack of hippocampal atrophy, we undertook a project to quantify the extent of GML in MCI patients as measured by MRI and verify whether the hippocampus continues to lose volume or not in AD. We employed neurocomputational methods that search the whole brain for differences and quantify the extent and asymmetry of brain GML (Ashburner and Friston, 2000; Ashburner et al., 2003; Grenander and Michael, 1998) or quantify global GM in a robust manner (Smith et al., 2002).

Materials and methods

Subjects with amnesic MCI (Petersen et al., 1999) and late-onset probable Alzheimer's disease (AD) (McKhann et al., 1984) were selected from consecutive referrals to an outpatient memory clinic in the period 2000–2002. To be included, every patient had to have received an MRI scan examination on the same scanner. The diagnosis of amnesic MCI was made if the subject had a score on the Global Deterioration Scale of 3 (Reisberg et al., 1982) and had impairment on memory tests as judged by a neuropsychologist. Specifically, the Petersen criteria were operationalized by including patients exhibiting memory complaints and neuropsychological evidence of a memory disorder >1.5 standard deviation below cutoff for normal aging, and no evidence for a deficit in any other cognitive domain, no activities of daily living (ADL) interference, and no clinical dementia. Healthy elderly controls (NCLR) were recruited among spouses or relatives of the patients.

Accordingly, MCI subjects with impairments in domains other than memory were excluded. Other exclusion criteria were history of depression, cardiovascular disease, or extensive vascular disease on MRI. In addition, subjects were excluded if the MRI scan did not allow VBM analysis.

MRI was performed on a 1.0-T Siemens Magnetom Impact Expert system (Siemens, Erlangen, Germany). Anatomical high-resolution scans were obtained as whole-brain T1-weighted 3D MPRAGE (magnetization prepared rapid acquisition gradient echo) volumes and were acquired in the coronal plane (TR, 15 ms; TE, 7 ms; TI, 300 ms; flip angle, 15°). Voxel sizes were $1 \times 1 \times 1.5$ mm. For the visual assessment of vascular burden, 2D FLAIR (Fluid Attenuated Inversion Recovery) images were acquired in the axial plane (TR, 9000 ms; TE, 105 ms; TI, 2200 ms; flip angle 180°).

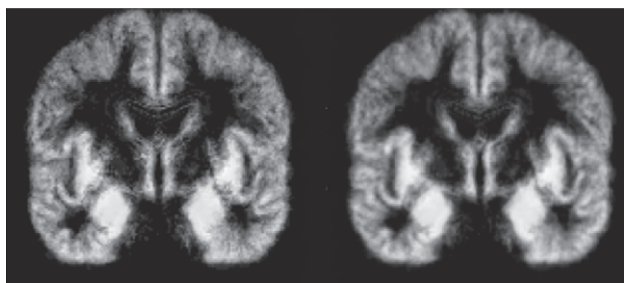


Fig. 1. Coronal sections of gray matter partitions of the NCLR group. On the left is the template derived from the usual VBM creation method and on the right is the template after transformation matrix averaging has occurred in the semi-Riemannian manifold. Note that the template on the right is much better defined, indicating that global anatomical variability has been reduced (a prerequisite for application of VBM).

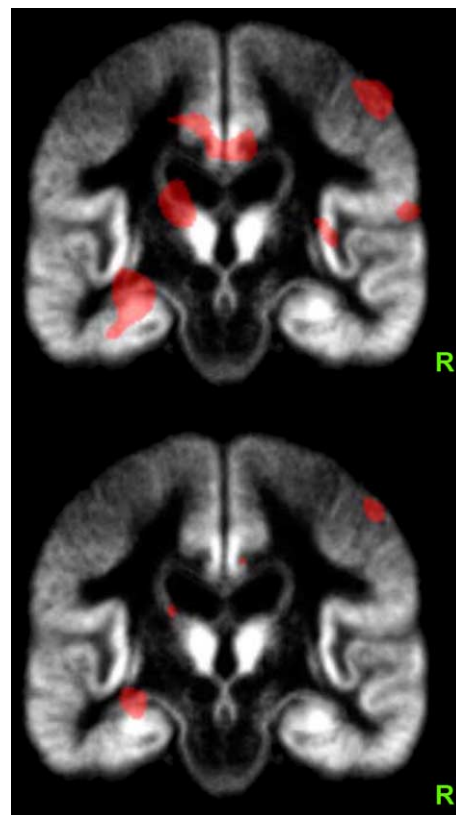


Fig. 2. Effect of threshold value on VBM results interpretation. In the upper panel, the T map was thresholded at $P = 0.0001$ and in the lower panel at $P = 0.001$. Notice that by lowering the threshold, the left MTL appears more atrophic and the right parietal association area and caudate head are enlarged. The cingulate cortex almost does not appear at all atrophic at the high threshold, but is obviously abnormal at the lower threshold.

Image processing

Data were analyzed at a global level using the cross-sectional version of Structural Image Evaluation, using Normalization, of Atrophy (SIENAX) as part of the FSL Oxford software suite (Smith et al., 2002): <http://www.fmrib.ox.ac.uk/fsl/>. For local-level analysis, we employed VBM methodology by SPM99 (<http://www.fil.ion.ucl.ac.uk/spm/>) running on MatLab 6.1 (The Mathworks, MA, USA). Additional special customized scripts in MatLab automated all VBM steps and ensured consistency. Image processing functions and visualization routines were coded in IDL 5.6 (Research Systems, Boulder, CO, USA). Advanced image registration was performed with AIR version 5 (freely available at: <http://bishopw.ion.ucla.edu/AIR5/>) (Woods, 2003). Skull extraction was performed with the Brain Extraction Tool (BET) from the FSL suite (Smith, 2002b). All processing steps were done on a Linux Workstation. All source code, templates, and extra scripts are freely available from the corresponding author upon request.

Global gray matter loss: SIENAX

The SIENAX algorithm was applied to estimate gray matter volumes corrected for skull size and is an algorithm that has been shown to perform well on differing slice thickness and sequences (Smith et al., 2002). SIENAX registers a scan to standard space, strips the skull, segments the gray matter, and uses the stripped

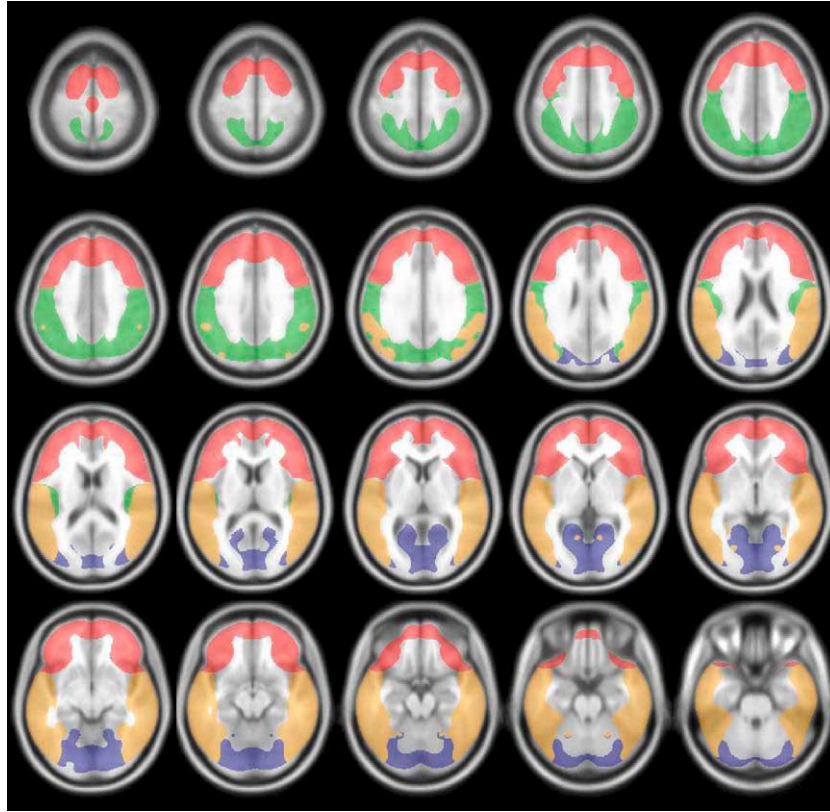


Fig. 3. Axial slices of the MNI standard brain with the automatic probability anatomical regions overlaid. These regions were used to estimate the statistical mass and gray matter lobar volume. Red = frontal lobe; green = parietal lobe; orange = temporal lobe; blue = occipital lobe.

skull to adjust the results for head size. In our implementation, we noticed that the skull extraction algorithm (BET) performed better if the scan was brought with rigid body registration to standard space first, because then the center of the sphere BET uses to expand is then in the center of the brain parenchyma.

Regional gray matter loss: optimized VBM with manifold projection

We applied optimized VBM with some modifications necessary for analyzing dementia MRI scans (Karas et al., 2003). Briefly, scans were registered twice: once to standard space and once to a local space. Local space is usually created by averaging the scans after they have been registered to standard space. Because there has been debate about misregistration influencing the results of VBM

Table 1
Demographics and clinical findings

	AD	MCI subgroup	NCLR
Sample size	33	22	14
Sex (F/M)	16/17	14/8	8/6
Age mean	73.9	71.4	70.2
(SD, range)	(3.8, 66–81)	(6.9, 53–79)	(9.8, 50–81)
MMSE score	21.1	26.4	27.8
(SD, range)	(5.3, 4–28)	(1.9, 24–30)	(1.7, 24–30)

Note: Ages were comparable for all groups at $P > 0.05$ (ANOVA). The MCI total and MCI subgroup did not differ for age ($P = 0.8$) and MMSE ($P = 0.7$).

MMSE scores between AD and NCLR differed at $P < 0.001$ (Kruskall–Wallis nonparametric test).

(Ashburner and Friston, 2001; Bookstein, 2001) and one of the assumptions for a correct VBM is reduced global anatomical variability (Ashburner and Friston, 2000), we enhanced the averaging process at the template-creation step by projecting the affine transformation matrices, which map all scans to a random scan from the group, to a semi-Riemannian manifold and averaging them there, thus creating a common transformation matrix for all scans (Woods, 2003). Subsequently, this matrix was applied to all scans and the process was iterated two times until maximum convergence was reached (semi-Riemannian manifolds and semi-Riemannian

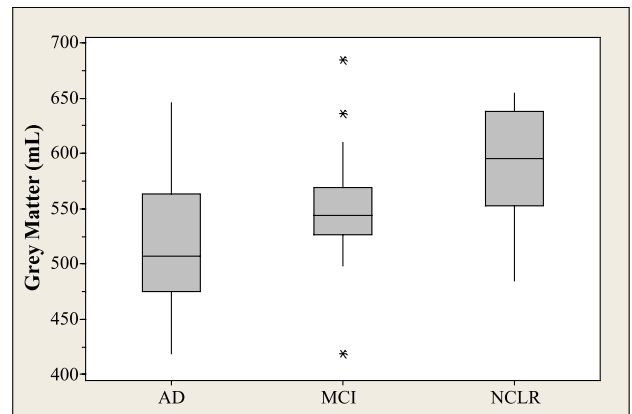


Fig. 4. Box plot of SIENAX-generated gray matter volumes. We notice that the AD group has lower gray matter volume than the MCI and the control group. Statistical analysis of the data showed that significance is present only between AD and controls.

geometry are advanced theoretical concepts of a multidimensional curved space, upon which the theory of relativity is based). This method removes registration bias arising from discrepancies between template and scan; it does not matter if some of the scans do not match the template very well: All scans will converge toward a ‘halfway’ common target (defined by the average transformation) spreading residual registration errors in an unbiased fashion.

Subsequently, gray matter, white matter, and cerebrospinal fluid were extracted and the gray matter intensity partitions were mapped by nonlinear registration ($5 \times 7 \times 5$ basis functions) to the common gray matter template and resampled at $1 \times 1 \times 1$ mm, to maximize use of structural information. Morphological opening was performed to correct for misclassified periventricular partial volume voxels (Karas et al., 2003). To accommodate for shrinking and

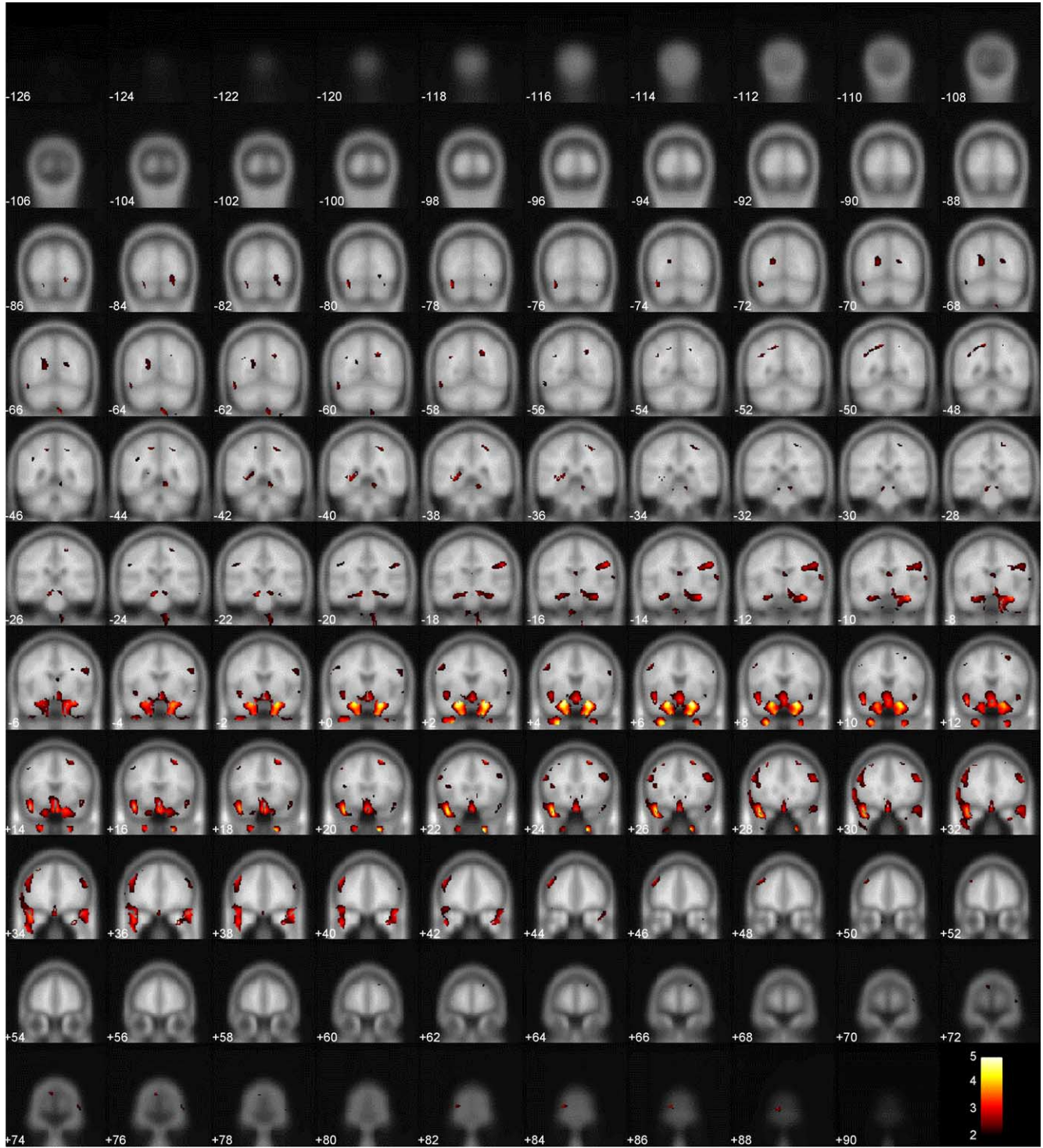


Fig. 5. MCI vs. NCLR at $P = 0.001$ (uncorrected). In MCI subjects, atrophy is confined in the MTL region without any major involvement of higher cortical areas.

expanding effects of the nonlinear registration part, we performed modulation (Ashburner and Friston, 2000). To evaluate registration success, we created a gray matter template with usual VBM methodology and one with transformation matrix projection. The latter template was much better defined compared to the usual VBM template, indicating reduced global anatomical variability (Fig. 1).

Statistical analysis of VBM

When performing statistics in a functional MRI (fMRI) experiment, one usually applies Gaussian kernel smoothing and the general linear model (Friston et al., 1996) to detect activations, i.e., changes in blood oxygen level dependent (BOLD) response. This statistical methodology was initially adopted en bloc by neurocomputational methods involving structural analysis. There are certain caveats though that might render this implementation troublesome (Thompson et al., 2003). The first drawback is the arbitrary setting of significant P values (or the equivalent T scores). Different thresholds reveal different structural changes. In Fig. 2, we demonstrate the absence of cingulate atrophy when setting the threshold to $P = 0.0001$ and presence of cingulate atrophy when using the lower threshold of $P = 0.001$ in the VBM AD vs. MCI comparison. The second drawback is the report of statistics according to cluster peak and extent. The peak is the maximum T score in a cluster and the extent is the number of connected voxels to that cluster. In a diffuse disease such as AD, cluster analysis would search for local maxima and form clusters around them, but leave widespread changes untouched unless they happened to have a local maximum. Thirdly, multiple-comparison correction methods have been used to adjust for statistical error but not for biological effect. It is evident that 3 million voxels of the same brain are not independent observations. That is especially true for voxels falling within the same Gaussian kernel. Conversely, if the same disease process causes atrophy of neighboring voxels, correcting for multiple comparisons would inevitably adjust for the assumed statistical type I error but also filter out the biological effect. Ultimately, one has to balance statistical significance with biological relevance.

To account the aforementioned issues, we applied the concept of statistical mass. Initially, traditional VBM statistics were calculated with SPM99 using the general linear model as previously described (Friston et al., 1996; Karas et al., 2003). Two-sample t tests were used to calculate the statistical contrasts. By comparing three groups, the number of contrasts one is allowed to perform is only two because the third contrast is already implied in the other two comparisons. Hence, we performed VBM analysis only for MCI vs. NCLR and MCI vs. AD. Subsequently, we partitioned the VBM statistical maps according to predefined anatomical regions and calculated the T -mean per anatomical region, thus determining the ‘statistical mass’ (SM) in the anatomical region (Bullmore et al., 1999). Appropriate choice of the anatomical regions to use was performed after the VBM maps were inspected visually to identify the atrophic areas. 3D standard anatomical probability maps (in MNI space) were used to mask the VBM maps (Fox and Lancaster, 1994; Hansen et al., 1999, 2001). The 3D anatomical probability maps range from 0 (null) to 1 (maximum) probability that a voxel belongs to the specified anatomical region. After visual inspection of the anatomical probability maps and taking into account that the gray matter volumes were smoothed with a kernel of 12 mm, a cutoff value of 0.5 for probability was used for voxel assignment (Fig. 3). We

could compare T -mean values between the two analyses because at relatively large samples, the corresponding T value for various P values varies only in the third decimal (e.g., at $P = 0.001$, the T value is 3.591 for 35 subjects and $T = 3.551$ for 40 subjects; Altman, 1991). Because a high statistical value may either arise because of true difference or low variability, we estimated gray matter subvolumes over the anatomical probability regions. Statistical mass results are expressed in Table 3 and differences in subvolumes are expressed as percent changes in Table 4.

Statistical analysis of SIENAX

SPSS 11 was used. Group comparisons for age and SIENAX means for GM were compared by ANOVA and differences between the means of the three groups were assessed by a post hoc Bonferroni test, when appropriate (nonsignificant homogeneity of the means and significant F value). Because of the ordinal nature of MMSE (an arbitrary rating scale), Kruskal–Wallis nonparametric test was performed by applying a Monte Carlo simulation of 10,000 sampling to test for differences between the three groups in MMSE scores.

Results

The total MCI population comprised of 68 subjects, 22 out of which fulfilled the inclusion criteria. The other two groups consisted of 33 subjects with AD and 14 control subjects. All groups were comparable for age at scanning. Demographics and clinical variables are presented in Table 1. To ensure that the selected MCI subpopulation was representative for the total MCI sample, we compared age and mini-mental state examination (MMSE, max score = 30; Folstein et al., 1975) between the included and excluded MCI subjects (no statistical significance, P for age = 0.8, P for MMSE = 0.7). As expected, the selected MCI subgroup comprised of individuals with very mild cognitive decline (mean MMSE of 26.4, range 24–30) and the AD group consisted of patients with mild cognitive decline (mean MMSE of 21.1, range 4–28).

MCI vs. NCLR

Comparing the three groups for global gray matter volume demonstrated a significant difference ($P < 0.0001$). At post hoc analysis, this appeared to be caused by the comparison of AD vs. NCLR (12% global GM volume reduction of GM, Bonferroni $P < 0.001$). The MCI group had a much smaller reduction of 6.5% of

Table 2
Global gray matter volume by disease group

	GM mean (SD) [ml]	GM loss as percent of NCLR [%]
AD	517.4 (58.2)	12.3
MCI	551.5 (52.1)	6.5
NCLR	590.0 (51.8)	–

Note: The three groups significantly differed in gray matter (GM) global volumes as determined by SIENAX [for a one-way ANOVA, $F(3,69) = 9.02$, $P < 0.0001$]. A Bonferroni post hoc test demonstrated significantly different global gray matter volumes for AD and NCLR ($P < 0.001$), but not between AD and MCI ($P = 0.08$), or MCI and NCLR ($P = 0.134$).

global GM volume compared to the NCLR subjects, which was not statistically significant (Bonferroni $P = 0.13$) reflecting the considerable overlap between the groups (Fig. 4). The two groups, however, markedly differed in terms of the pattern of regional gray matter (Fig. 5; Tables 3 and 4). On a lobar level, the most significant difference in MCI subjects compared to NCLR subjects was seen in the parietal lobes followed by the frontal lobes. Focusing on a more detailed level, the structure most affected in subjects with MCI was the thalamus bilaterally followed by the superior temporal cortex

bilaterally, the left insula, and the hippocampus bilaterally. Compared to the NCLR subjects, MCI subjects had only modest SM differences in the parietal association areas, the retrosplenial cingulate cortex, and the temporo-parietal cortex.

MCI vs. AD

The difference in gray matter volume between MCI and AD subjects was 6.2%, which did not reach statistical significance ($P =$

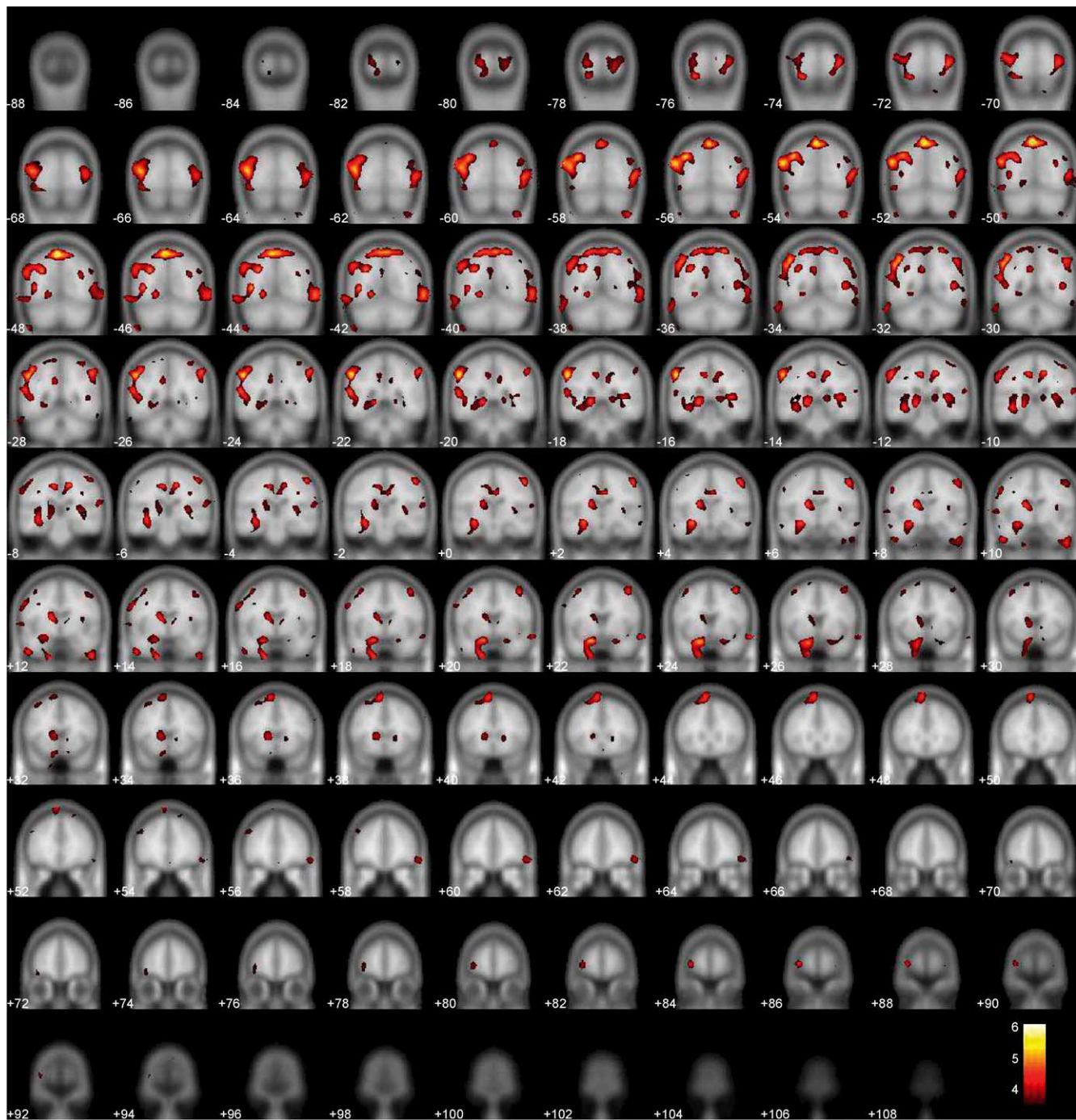


Fig. 6. AD vs. MCI at $P = 0.001$ (uncorrected). AD subjects demonstrate more atrophy in the medial temporal lobe, but also in the parietal cortex and cingulate cortex. The quantified VBM maps for these findings indeed confirmed the visual appearance of the VBM maps without the need to set threshold and consequently introduce bias.

0.08; Table 2). VBM analysis revealed clear differences in SM in several brain regions (Fig. 6; Tables 3 and 4). Subjects with AD showed a greater SM in the temporal and parietal lobes compared to subjects with MCI. Subjects with AD also showed a greater SM of the frontal and occipital lobes but this difference was less pronounced. On a more detailed level, the structure that had the greatest SM in AD patients compared to MCI patients was the left amygdala, closely followed by the rest of the MTL structures. The left insula was not more involved in AD compared to MCI patients. SM in AD patients was more severe at the left side than at the right side (with the exception of the insula). Parietal association areas demonstrated a high SM, comparable to the levels seen in the MTL. Involvement of the cingulate cortex was also noted, with the retrosplenial cingulate equally involved as the parietal association and with the anterior cingulate a little less.

Discussion

In the current study, we used two different methodologies to quantify gray matter differences in MCI patients compared with

Table 3
Statistical mass (standard deviation) by anatomical region

Label	Corrected mean <i>T</i> value			
	NCLR vs. MCI		MCI vs. AD	
	L	R	L	R
<i>Lobes</i>				
Frontal lobe	0.58 (0.40)	0.54 (0.37)	1.45 (0.49)	1.33 (0.45)
Temporal lobe	0.47 (0.29)	0.39 (0.27)	2.06 (0.58)	2.20 (0.63)
Parietal lobe	0.74 (0.370)	0.77 (0.43)	2.09 (0.80)	1.95 (0.59)
Occipital lobe	0.44 (0.29)	0.31 (0.20)	1.77 (0.68)	1.41 (0.68)
<i>MTL, basal ganglia, and insula</i>				
Amygdala	1.07 (0.51)	1.26 (0.74)	3.17 (0.66)	2.35 (0.62)
Hippocampus	1.14 (0.72)	1.32 (0.67)	2.12 (0.79)	1.47 (0.62)
Thalamus	1.81 (0.57)	1.49 (0.64)	2.20 (1.26)	1.84 (0.92)
Caudate head	0.95 (0.67)	0.74 (0.50)	2.28 (0.75)	1.94 (0.49)
Insula	1.52 (0.74)	0.93 (0.54)	1.64 (0.66)	1.97 (0.52)
Superior temporal cortex	1.61 (0.78)	1.37 (0.46)	2.06 (0.50)	2.39 (0.39)
<i>Cortical association areas and cingulate</i>				
Parietal association	0.68 (0.38)	0.62 (0.36)	2.69 (0.95)	2.16 (0.88)
Retrosplenial cingulate	0.74 (0.35)	0.57 (0.28)	2.61 (1.02)	1.73 (0.77)
Anterior cingulate	0.25 (0.15)	0.32 (0.19)	1.99 (0.92)	1.37 (0.41)

Note: These values are quantitative *T* statistics and should be interpreted as absolute values. For example, the *T* statistic for the left amygdala in the MCI-AD comparison is 3.17 and the corresponding value for the MCI-NCLR comparison is 1.07, indicating that the degree of atrophy in the amygdala in the first case is roughly three times of that in the second case.

Table 4
Mean percentage differences of gray matter of anatomical regions

Label	Mean percentage difference (%)			
	NCLR vs. MCI		MCI vs. AD	
	L	R	L	R
<i>Lobes</i>				
Frontal lobe	4.5	3.1	11.1	9.4
Temporal lobe	1.7	0.8	10.9	11.2
Parietal lobe	6.3	7.2	13.1	12.4
Occipital lobe	0.5	-0.2	12.9	11.2
<i>MTL, basal ganglia, and insula</i>				
Amygdala	3.3	4.1	10.7	7.6
Hippocampus	4.9	5.9	7.9	5.5
Thalamus	13.4	12.4	14.1	14.2
Caudate head	4.6	4.1	10.5	10.6
Insula	4.6	3.2	6.9	8.2
Superior temporal cortex	7.2	6.4	8.5	10.7
<i>Cortical association areas and cingulate</i>				
Parietal association	2.3	3.0	18.7	16
Retrosplenial cingulate	3.1	3.5	7.3	5.9
Anterior cingulate	-0.2	1.2	9.2	8.1

normal controls and AD patients. While global gray matter volume did not clearly distinguish MCI from the other two groups, spatially varying differences were detected between groups, whereby the MCI group differed from the NCLR group in terms of atrophy of the MTL region, thalamus, and insula. By contrast, GM losses in the parietal association cortices and cingulate cortex were hallmarks of the AD group when compared to MCI. The AD subjects also had more atrophy in the MTL, indicating an ongoing atrophic process in that area.

Atrophy of the anterior cingulate, postulated to be an early marker of AD (Killiany et al., 2000), was not a distinctive feature when MCI patients were compared to NCLR, but was quite evident when the AD group was compared to MCI. Interestingly, in the study by Killiany et al., posterior cingulate involvement was only evident when MCI was compared to controls, but not between AD and MCI. The differences between these studies may be technical, but also differences in patient selection, with our MCI group being closer to NCLR than AD for their MMSE scores.

In a recent VBM study, a similar pattern of parietal atrophy was found in Alzheimer's patients compared to MCI patients (Chetelat et al., 2002). That study did not reveal any hippocampal atrophy in the transitional stage from MCI to AD, suggesting a plateau had been reached, or even postulating that neural plasticity compensated for the volume loss (Chetelat et al., 2002). In our study though, the hippocampus still demonstrated atrophy in the AD group. This discrepancy may be due to the fact that in the study by Chetelat et al., the hippocampal atrophy might have just been under the arbitrary significance level set by the authors, or due to differences in disease severity of the MCI populations.

In a previous study we conducted with moderate to severe Alzheimer's patients, we observed a close adherence to the Braak stages (Karas et al., 2003): MTL atrophy accompanied by diffuse neocortical atrophy with the exception of the occipital cortex and the sensorimotor strip. In the current study, we did not aim to look at cumulative atrophy in AD compared to controls, but atrophy in the regions that would distinguish MCI from AD and NCLR. We noticed that atrophy patterns still seemed to adhere to the Braak

staging, with the exception of the thalamus. Early thalamic involvement, not a characteristic of the Braak staging, has been observed in recent metabolic hypoperfusion studies (Callen et al., 2002; Chetelat et al., 2003b; Nestor et al., 2003) and reported as a discriminative factor of AD in recent meta-analysis (Zakzanis et al., 2003), but manual outlining of the thalamus is necessary to confirm this finding. Brain atrophy or hypometabolism might exhibit themselves in areas further away from the expected Braak pattern; recently, it has been reported that parietal association metabolic impairment differentiates AD from MCI (Chetelat et al., 2003b) and that these metabolic reductions might even exceed gray matter volume losses (De Santi et al., 2001). Our current study, on the other hand, using a sample of comparable age and MMSE scores with the study of de Santi et al., demonstrated possible neocortical GML in the AD group, but unfortunately we did not have PET data to compare the difference in magnitude. Arguably, the gray matter measurements of the De Santi group were not optimally tuned to evaluate cortical atrophy (gyral–sulcal variability makes it very difficult to perform accurate region of interest measurements in cortical areas) and accordingly find a correlation with metabolic impairment. Interestingly, another recent study (Chetelat et al., 2003a) measured the dissociation between hypometabolism on FDG-PET and VBM of MRI in MCI and correlated encoding and retrieval findings with only the hippocampal loss (VBM) and posterior cingulate hypometabolism (FDG-PET). It remains unclear why the VBM study of Chetelat et al. was unable to demonstrate posterior cingulate involvement, while in our case it was possible. Methodological differences in the VBM implementation or focusing only on the encoding–retrieving task might explain the discrepancy.

Our results agree with the findings of a recent meta-analysis of volumetric studies in AD (Zakzanis et al., 2003), where it was found that disease duration of less than 4 years was mainly characterized by atrophy in the MTL region, while disease duration of more than 4 years (hence higher probability of having true AD clinical picture) showed extension to other structures like the caudate nucleus, parietal-occipital regions, and frontal and parietal lobes.

Our findings indicate a laterality trend of the atrophic process. The AD group demonstrated more left-sided atrophy. This comes in accordance with several VBM studies (Baron et al., 2001; Karas et al., 2003), sulcal-warping studies (Thompson et al., 2001, 2003), SPECT and PET studies (Duara et al., 1986; Johnson et al., 1998; Loewenstein et al., 1989), which support left greater than right hemispheric involvement in AD. The right hemisphere has been described as having a “time lag” in demonstrating atrophy (Thompson et al., 2003). The finding of greater right medial temporal atrophy in MCI is intriguing. It is known that healthy brain is asymmetrical in structure and function (Toga and Thompson, 2003), with the right hippocampus approximately 5% larger than the left (Jack et al., 2003). It is unclear why our MCI group demonstrated inverted laterality. A recent study suggested that disease duration of less than 2 years is associated with larger left than right hippocampi in MCI and AD patients (Bigler et al., 2002). It remains to be elucidated, in case laterality inversion does take place, whether a time frame of 2 years forms a pivotal point.

A drawback of the implementation of regionalized statistical mass, via the MNI standard masks, is that distorted pathology might “pull” structures out of the anatomical mask, thus creating artificially reduced gray matter. That might be especially true in the case of AD pathology with known ventricular expansion. For this

reason, we opted for empirically wider anatomical masks, which would ensure the structures of interest fall within the mask. Another weakness of this study is its cross-sectional nature and the temporal pattern of evolution suggested by the two separate comparisons needs to be validated in a longitudinal study where each subject serves as its own control in a framework of high-dimensional transforms and voxel-compression mapping (Scahill et al., 2002; Schott et al., 2003). An additional limitation is that some of the MCI subjects may not develop AD but may have MCI due to other causes. Therefore, the differences between NCLR and MCI subjects who will convert to AD may have been underestimated (and those between MCI and AD overestimated).

In summary, while MCI might indeed lie empirically ‘halfway’ between AD and NCLR, as indicated by global GM measurements, spatially varying anatomical areas are involved in this transitional phase, suggesting that early changes in AD involve the MTL, thalamus, and insula, while established AD also involves parietal association areas and cingulate.

Acknowledgments

G. Karas is the recipient of Grant 2001-014 by the “Stichting Alzheimer Nederland” and S.A.R.B. Rombouts is the recipient of Grant H00.17 from “Hersenstichting Nederland”.

References

- Altman, D.G., 1991. *Practical Statistics for Medical Research*. Chapman & Hall, London.
- Ashburner, J., Friston, K.J., 2000. Voxel-based morphometry—the methods. *NeuroImage* 11, 805–821.
- Ashburner, J., Friston, K.J., 2001. Why voxel-based morphometry should be used. *NeuroImage* 14, 1238–1243.
- Ashburner, J., Csernansky, J.G., Davatzikos, C., Fox, N.C., Frisoni, G.B., Thompson, A.J., 2003. Computer-assisted imaging to assess brain structure in healthy and diseased brains. *Lancet Neurol.* 2, 79–88.
- Baron, J.C., Chetelat, G., Desgranges, B., Perchev, G., Landeau, B., de la Sayette, V., Eustache, F., 2001. In vivo mapping of gray matter loss with voxel-based morphometry in mild Alzheimer’s disease. *NeuroImage* 14, 298–309.
- Bigler, E.D., Tate, D.F., Miller, M.J., Rice, S.A., Hessel, C.D., Earl, H.D., Tschanz, J.T., Plassman, B., Welsh-Bohmer, K.A., 2002. Dementia, asymmetry of temporal lobe structures, and apolipoprotein E genotype: relationships to cerebral atrophy and neuropsychological impairment. *J. Int. Neuropsychol. Soc.* 8, 925–933.
- Bookstein, F.L., 2001. “Voxel-based morphometry” should not be used with imperfectly registered images. *NeuroImage* 14, 1454–1462.
- Braak, H., Braak, E., 1991. Neuropathological staging of Alzheimer-related changes. *Acta Neuropathol. (Berl)* 82, 239–259.
- Bullmore, E.T., Suckling, J., Overmeyer, S., Rabe-Hesketh, S., Taylor, E., Brammer, M.J., 1999. Global, voxel, and cluster tests, by theory and permutation, for a difference between two groups of structural MR images of the brain. *IEEE Trans. Med. Imag.* 18, 32–42.
- Callen, D.J., Black, S.E., Caldwell, C.B., 2002. Limbic system perfusion in Alzheimer’s disease measured by MRI-coregistered HMPAO SPET. *Eur. J. Nucl. Med. Mol. Imaging* 29, 899–906.
- Chetelat, G., Desgranges, B., De La Sayette, V., Viader, F., Eustache, F., Baron, J.C., 2002. Mapping gray matter loss with voxel-based morphometry in mild cognitive impairment. *NeuroReport* 13, 1939–1943.
- Chetelat, G., Desgranges, B., De La Sayette, V., Viader, F., Berkouk, K., Landeau, B., Lalevee, C., Le Doze, F., Dupuy, B., Hannequin, D.,

- Baron, J.C., Eustache, F., 2003. Dissociating atrophy and hypometabolism impact on episodic memory in mild cognitive impairment. *Brain* 126, 1955–1967.
- Chetelat, G., Desgranges, B., De La Sayette, V., Viader, F., Eustache, F., Baron, J.C., 2003b. Mild cognitive impairment: can FDG-PET predict who is to rapidly convert to Alzheimer's disease? *Neurology* 60, 1374–1377.
- De Santi, S., de Leon, M.J., Rusinek, H., Convit, A., Tarshish, C.Y., Roche, A., Tsui, W.H., Kandil, E., Boppana, M., Daisley, K., Wang, G.J., Schlyer, D., Fowler, J., 2001. Hippocampal formation glucose metabolism and volume losses in MCI and AD. *Neurobiol. Aging* 22, 529–539.
- Delacourte, A., David, J.P., Sergeant, N., Buee, L., Wattez, A., Vermersch, P., Ghozali, F., Fallet-Bianco, C., Pasquier, F., Lebert, F., Petit, H., Di Menza, C., 1999. The biochemical pathway of neurofibrillary degeneration in aging and Alzheimer's disease. *Neurology* 52, 1158–1165.
- Duara, R., Grady, C., Haxby, J., Sundaram, M., Cutler, N.R., Heston, L., Moore, A., Schlageter, N., Larson, S., Rapoport, S.I., 1986. Positron emission tomography in Alzheimer's disease. *Neurology* 36, 879–887.
- Folstein, M.F., Folstein, S.E., McHugh, P.R., 1975. "Mini-mental state". A practical method for grading the cognitive state of patients for the clinician. *J. Psychiatr. Res.* 12, 189–198.
- Fox, P.T., Lancaster, J.L., 1994. Neuroscience on the net. *Science* 266, 994–996.
- Friston, K.J., Holmes, A., Poline, J.B., Price, C.J., Frith, C.D., 1996. Detecting activations in PET and fMRI: levels of inference and power. *NeuroImage* 4, 223–235.
- Gomez-Isla, T., Hollister, R., West, H., Mui, S., Growdon, J.H., Petersen, R.C., Parisi, J.E., Hyman, B.T., 1997. Neuronal loss correlates with but exceeds neurofibrillary tangles in Alzheimer's disease. *Ann. Neurol.* 41, 17–24.
- Grenander, U., Michael, M., 1998. Computational anatomy: an emerging discipline. *Q. Appl. Math.* 56, 617–694.
- Hansen, L.A., Nielsen, F.A., Toft, P., Liptrot, M.G., Goutte, C., Strother, S.C., Lange, N., Gade, A., Rottenberg, D.A., Paulson, O.B., 1999. "lyngby"—a modeler's Matlab toolbox for spatio-temporal analysis of functional Neuroimages. *NeuroImage* 9, S241.
- Hansen, L.K., Nielsen, F.A., Strother, S.C., Lange, N., 2001. Consensus inference in neuroimaging. *NeuroImage* 13, 1212–1218.
- Jack Jr., C.R., Slomkowski, M., Gracon, S., Hoover, T.M., Felmlee, J.P., Stewart, K., Xu, Y., Shiung, M., O'Brien, P.C., Cha, R., Knopman, D., Petersen, R.C., 2003. MRI as a biomarker of disease progression in a therapeutic trial of milameline for AD. *Neurology* 60, 253–260.
- Johnson, K.A., Jones, K., Holman, B.L., Becker, J.A., Spiers, P.A., Satlin, A., Albert, M.S., 1998. Preclinical prediction of Alzheimer's disease using SPECT. *Neurology* 50, 1563–1571.
- Karas, G.B., Burton, E.J., Rombouts, S.A., van Schijndel, R.A., O'Brien, J.T., Scheltens, P., McKeith, I.G., Williams, D., Ballard, C., Barkhof, F., 2003. A comprehensive study of gray matter loss in patients with Alzheimer's disease using optimized voxel-based morphometry. *NeuroImage* 18, 895–907.
- Killiany, R.J., Gomez-Isla, T., Moss, M., Kikinis, R., Sandor, T., Jolesz, F., Tanzi, R., Jones, K., Hyman, B.T., Albert, M.S., 2000. Use of structural magnetic resonance imaging to predict who will get Alzheimer's disease. *Ann. Neurol.* 47, 430–439.
- Loewenstein, D.A., Barker, W.W., Chang, J.Y., Apicella, A., Yoshii, F., Kothari, P., Levin, B., Duara, R., 1989. Predominant left hemisphere metabolic dysfunction in dementia. *Arch. Neurol.* 46, 146–152.
- McKhann, G., Drachman, D., Folstein, M., Katzman, R., Price, D., Stadlan, E.M., 1984. Clinical diagnosis of Alzheimer's disease: report of the NINCDS-ADRDA Work Group under the auspices of Department of Health and Human Services Task Force on Alzheimer's Disease. *Neurology* 34, 939–944.
- Mega, M.S., Chen, S.S., Thompson, P.M., Woods, R.P., Karaca, T.J., Tiwari, A., Vinters, H.V., Small, G.W., Toga, A.W., 1997. Mapping histology to metabolism: coregistration of stained whole-brain sections to premortem PET in Alzheimer's disease. *NeuroImage* 5, 147–153.
- Mega, M.S., Chu, T., Mazziotta, J.C., Trivedi, K.H., Thompson, P.M., Shah, A., Cole, G., Frautschy, S.A., Toga, A.W., 1999. Mapping biochemistry to metabolism: FDG-PET and amyloid burden in Alzheimer's disease. *NeuroReport* 10, 2911–2917.
- Nestor, P.J., Fryer, T.D., Smielewski, P., Hodges, J.R., 2003. Limbic hypometabolism in Alzheimer's disease and mild cognitive impairment. *Ann. Neurol.* 54, 343–351.
- Petersen, R.C., Smith, G.E., Waring, S.C., Ivnik, R.J., Tangalos, E.G., Kokmen, E., 1999. Mild cognitive impairment: clinical characterization and outcome. *Arch. Neurol.* 56, 303–308.
- Petersen, R.C., Doody, R., Kurz, A., Mohs, R.C., Morris, J.C., Rabins, P.V., Ritchie, K., Rossor, M., Thal, L., Winblad, B., 2001. Current concepts in mild cognitive impairment. *Arch. Neurol.* 58, 1985–1992.
- Reisberg, B., Ferris, S.H., de Leon, M.J., Crook, T., 1982. The global deterioration scale for assessment of primary degenerative dementia. *Am. J. Psychiatry* 139, 1136–1139.
- Scahill, R.I., Schott, J.M., Stevens, J.M., Rossor, M.N., Fox, N.C., 2002. Mapping the evolution of regional atrophy in Alzheimer's disease: unbiased analysis of fluid-registered serial MRI. *Proc. Natl. Acad. Sci. U. S. A.* 99, 4703–4707.
- Schott, J.M., Fox, N.C., Frost, C., Scahill, R.I., Janssen, J.C., Chan, D., Jenkins, R., Rossor, M.N., 2003. Assessing the onset of structural change in familial Alzheimer's disease. *Ann. Neurol.* 53, 181–188.
- Smith, A.D., 2002a. Imaging the progression of Alzheimer pathology through the brain. *Proc. Natl. Acad. Sci. U. S. A.* 99, 4135–4137.
- Smith, S.M., 2002b. Fast robust automated brain extraction. *Hum. Brain Mapp.* 17, 143–155.
- Smith, S.M., Zhang, Y., Jenkinson, M., Chen, J., Matthews, P.M., Federico, A., De Stefano, N., 2002. Accurate, robust, and automated longitudinal and cross-sectional brain change analysis. *NeuroImage* 17, 479–489.
- Thompson, P.M., Mega, M.S., Woods, R.P., Zoumalan, C.I., Lindshield, C.J., Blanton, R.E., Moussai, J., Holmes, C.J., Cummings, J.L., Toga, A.W., 2001. Cortical change in Alzheimer's disease detected with a disease-specific population-based brain atlas. *Cereb. Cortex* 11, 1–16.
- Thompson, P.M., Hayashi, K.M., de Zubicaray, G., Janke, A.L., Rose, S.E., Semple, J., Herman, D., Hong, M.S., Dittmer, S.S., Doddrell, D.M., Toga, A.W., 2003. Dynamics of gray matter loss in normal aging and Alzheimer's disease. *J. Neurosci.* 23, 994–1005.
- Toga, A.W., Thompson, P.M., 2003. Mapping brain asymmetry. *Nat. Rev., Neurosci.* 4, 37–48.
- Visser, P.J., Scheltens, P., Verhey, F.R., Schmand, B., Launer, L.J., Jolles, J., Jonker, C., 1999. Medial temporal lobe atrophy and memory dysfunction as predictors for dementia in subjects with mild cognitive impairment. *J. Neurol.* 246, 477–485.
- Woods, R.P., 2003. Characterizing volume and surface deformations in an atlas framework: theory, applications, and implementation. *NeuroImage* 18, 769–788.
- Zakzanis, K.K., Graham, S.J., Campbell, Z., 2003. A meta-analysis of structural and functional brain imaging in dementia of the Alzheimer's type: a neuroimaging profile. *Neuropsychol. Rev.* 13, 1–18.